Int J Adv Manuf Technol (2017) 89:2387–2397
DOI 10.1007/s00170-016-9263-3

ORIGINAL ARTICLE

Mechanical property parametric appraisal of fused deposition modeling parts based on the gray Taguchi method

Xinhua Liu[1] · **Mingshan Zhang**[1] · **Shengpeng Li**[2] · **Lei Si**[1] · **Junquan Peng**[1] · **Yuan Hu**[1]

Received: 3 May 2016 / Accepted: 1 August 2016 / Published online: 12 August 2016

Abstract The mechanical properties of a fused deposition modeling (FDM) process product are greatly influenced by many process parameters. The identified parameters namely deposition orientation, layer thickness and deposition style, raster width, and raster gap are more significant factors contributing to the strength of a FDM product. In this paper, tensile strength, flexural strength, and impact strength are considered as three evaluation indexes to characterize the mechanical properties of a FDM part. An experimental research approach based on the Taguchi method was presented and some special specimens were designed. The influences of the five parameters on the three evaluation indexes were analyzed by the use of analysis of variance (ANOVA). Finally, based on the gray relational analysis, a set of optimal process parameter combination was obtained to optimize comprehensive mechanical properties of FDM parts.

Keywords FDM parts · Mechanical property · Process parameter optimization · Taguchi technique · Gray relational analysis

1 Introduction

Rapid prototyping technology (RPT) is the collective name of a set of different technologies and processes used to manufacture models directly from three-dimensional computer-aided design model by constructing them layer by layer. As a manufacturing technology to fabricate physical models or parts rapidly, RPT is widely applied in the machinery, aerospace, construction, medical, cultural, and other fields [1–3]. Different from traditional machining methods, RPT adopts the additive manufacturing processes [4]. It modifies the geometry of a mass of material by removing parts of the material until the final shape is achieved [5]. The most significant feature of rapid prototyping is the ability to manufacture parts of any complexity of geometry entirely without the need of conventional tooling and services of skilled model makers. The representative processes of RPT are fused deposition modeling (FDM), stereo lithography apparatus (SLA), laminated object manufacturing (LOM), selective laser sintering (SLS), 3D printing (3DP), etc.

FDM is a typical example of the rapid prototyping (RP) processes. In recent years, simplicity of operation, inexpensive machinery, and durability of parts result in its great development. The FDM is able to produce prototypes from plastic materials, such as acrylonitrile butadiene styrene (ABS) or polylactic acid (PLA). In FDM process, the hot-melting filament feedstock is heated up to their melting point temperature and then deposited by an extrusion head. Meanwhile, the extrusion head can be moved in both horizontal and vertical directions by a numerically controlled mechanism. The nozzle follows a tool path which is controlled by computer-aided manufacturing (CAM) software, and the part is built from the bottom up, one layer at a time [6, 7].

Although FDM is an efficient technology, some drawbacks still exist. One of the drawbacks of FDM parts is the strength limitation. As a consequence, the practical application of components processed by the FDM is

✉ Xinhua Liu
l_xinhua_2006@126.com

[1] School of Mechanical and Electrical Engineering, China University of Mining & Technology, Xuzhou, China

[2] China Ship Scientific Research Center, Wuxi, China

limited to low-loaded products whose failures do not lead to severe effects. There is a main trend to apply the molding parts directly to the actual production and life. Especially in the field of medical application as patient's prosthetic limb, high load carrying capacity of the component is urgently required. Since the final mechanical properties of parts obtained by means of the FDM process are influenced by a large amount of production parameters which are difficult to combine, it is absolutely important to study the influence of various process parameters on the mechanical properties of FDM products and conduct the optimization so that improvement can be made through selection of best setting.

The rest of this paper is organized as follows: Some related works are outlined based on literature in Section 2. The experimental research is proposed in Section 3. The experimental optimization with the gray relational analysis is elaborated in Section 4. The conclusions and future work are summarized in Section 5.

2 Literature review

Aiming at improve mechanical properties of molding parts, several attempts have been made to study influence of various process parameters on it. The study of Es Said et al. [8] shows that raster orientation causes alignment of polymer molecules along the direction of deposition during fabrication and influence tensile, flexural, and impact strengths. In the study of Hutmacher D W et al. [9], the forming structures of FDM parts were analyzed from the micro perspective. It is found that the pore volume and structure and the porosity of the scaffolds were mainly defined by the setting of the computer-controlled FDM machine parameters and the honeycomb design resulted in good mechanical properties. In Ahn S H et al. [10], they evaluated the effect that FDM build parameters have on anisotropic material properties. With the use of a design of experiment (DOE) approach, they pointed out that process parameters such as air gap and raster orientation significantly affect the tensile strength of FDM part as compared to other parameters like raster width, model temperature, and color. Lee et al. [11] performed experiments on cylindrical parts made with FDM, 3D printer, and nanocomposite deposition (NCDS) to study the effect of build direction on compressive strength. Experimental result that compressive strength is 11.6 % higher for axial FDM specimen as compared to transverse FDM specimen shows diagonal specimen possesses maximum compressive strength in comparison to axial specimen. Bellehumeur C T et al. [12] investigated the mechanisms controlling the bond formation among extruded polymer filaments in the FDM process. The bonding phenomenon is thermally driven and ultimately determines the integrity and mechanical properties of the resultant prototypes. In Jaya Christiyan K G et al. [13], samples with different layer thickness and printing speed were prepared. Based on the experimental results, it is suggested that low printing speed and low layer thickness have resulted in maximum tensile and flexural strengths, as compared to all the other process parameter samples.

Many theoretical models and numerical analysis methods had been adopted to improve the mechanical properties. In Khan ZA et al. [14], an orthogonal array, main effect, the signal-to-noise (S/N) ratio, and ANOVA were employed to investigate the process parameters in order to achieve optimum elastic performance of a compliant ABS prototype so as to get maximum throwing distance from the prototype. It was found that FDM parameters, layer thickness, raster angle, and air gap significantly affect the elastic performance of the compliant ABS prototype. Croccolo D et al. [15] developed an analytical model, which is able to predict the strength and the stiffness properties, based on the number of contours deposited around the component edge and on the setting of the other main parameters of the deposition process. The effectiveness of the theoretical model has been verified by comparison to a significant number of experimental results, with mean errors of about 4 %. Kotlinski J et al. [16] summarized the common mechanical property indexes of rapid prototyping materials. The study that includes the ranges of properties allows choosing the material to build an object without familiarizing with particular time-consuming manufacturers' offers. In Anoop Kumar Sood et al.[17], five important process parameters such as layer thickness, orientation, raster angle, raster width, and air gap were considered to study their influence on tensile, flexural, and impact strengths of test specimen. Empirical models relating response and process parameters were developed and the model was tested using ANOVA.

These works reveal that the mechanical properties of FDM parts can be significantly improved with proper building parameters without incurring additional expenses for changing hardware and software. Although many process measures, theoretical models, and numerical analysis methods have been proposed to increase the part strength of FDM parts in above literatures, systematic experimental study has not been done to provide the optimum combination of process parameters. Based on the past research on the part strength in the FDM process, this paper tries to tackle this problem. In this paper, some experiments based on the Taguchi method were provided, and the optimal combination of the five parameters was obtained through the gray relational analysis to

Table 1 Factors and their levels

Factors	Symbol	Measuring unit	Levels		
			1	2	3
Deposition orientation	A	°	0	30	60
Layer thickness	B	mm	0.1	0.2	0.3
Deposition style	C	—	0	0/90	+45/−45
Raster width	D	mm	0.4	0.45	0.5
Raster gap	E	mm	–0.1	0	0.1

optimize the comprehensive mechanical properties of FDM parts.

3 The experimental research approach

3.1 Process parameter selection

There are many factors which influence the mechanical properties of FDM parts, such as molding equipment performance, molding material properties, processing conditions, after treatment process measures, and molding process parameters. This paper mainly explores the influence of process parameters on the mechanical properties of parts. Based on previous research results [10, 18] and practical experience in processing, the deposition orientation (a), layer thickness (b), deposition style (c), raster width (d), and raster gap (e) are selected as the experimental factors to explore the effect of these parameters on the mechanical properties of parts. The values of each level for these factors are determined according to the value recommended by the past experience of equipment manufacturer. The selected factors and their levels are shown in Table 1 and the specific implications of these factors are described as follows.

(a) Deposition orientation. It is the position where the part is built. Different position orientations will lead to different cross sections curing structure at the same location of molding parts. θ represents the deposition orientation angle displayed in Fig. 1.

(b) Layer thickness. It is the thickness of layer deposited by nozzle and depends upon the type of nozzle used.

(c) Deposition style. It is the pattern of raster used to fill the interior regions of the PLA part in accordance with the outline information of the cross section. The schematic diagram of three typical filling styles, including long-raster (0°), long-short-raster (+90°/0°), and staggered-raster (+45°/−45°), are exhibited in Fig. 2. The angle value is the included angle between the filling line and *ox* axis.

(d) Raster width. It is the width of raster pattern used to fill interior regions of part.

(e) Raster gap. It is the gap between two adjacent rasters on the same layer.

3.2 Experimental specimen preparation

Special test specimens for tensile strength experiment, flexural strength experiment, and impact strength experiment are designed in this section. The CAD model of specimen is modeled in Pro/ENGINEER Wildfire 5.0 and exported as a Standard Template Library (STL) file, which is imported to the FDM software in order to form date files. The specimens for each experiment are fabricated using the Desktop 3D Printer MakerBot Replicator 2, and the filament feedstock used for fabricating test specimen is PLA.

1. Specimen for tensile strength experiment
   Tensile specimen is designed as GB/T 1040.2-2006 in this paper. Its schematic diagram and dimensions are shown in Fig. 3 and Table 2.
2. Specimen for flexural strength experiment
   Flexural specimen is built based on GB/T 9341-2008. The recommended dimensional details of the test specimen are given in Fig. 4. The length $l = 80 \pm 2$ mm, width $b = 10.0 \pm 0.2$ mm, and thickness $h = 4.0$ mm ± 0.2 mm.

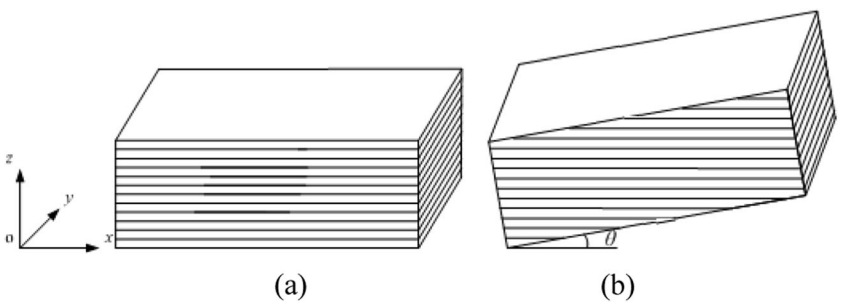

Fig. 1 The cross section (**a**) and different deposition orientations (**b**)

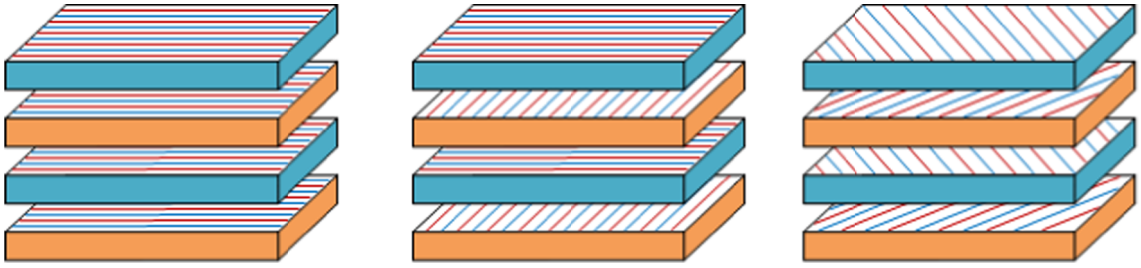

Fig. 2 Schematic diagram of deposition style

3. Specimen for impact strength experiment

   The specimen designed for impact strength experiment is based on GB/T 1043.1-2008. To ensure the accuracy of the specimen, unnotched specimen is adopted in this paper. Its shape and size are the same with the flexural experiment specimen in Fig. 4.

3.3 Experiment procedure

3.3.1 Experiment for tensile strength

If the classical design of experiment (DOE) method is used to experimental design, it would require a total of 3^5 (243) experimental runs. The Taguchi method of experimental design provides a simple, efficient, and systematic approach, called fractional factorial method for minimizing the number of total experiment runs [19].

The orthogonal array is employed for the Taguchi method as the experimental analysis basis. By the previous research results and the practical processing experience, the deposition orientation has great influence on the mechanical properties of the parts [20, 21]. Hence, the interactions of other parameters with deposition orientation are also taken into consideration in this paper, such as A × B, A × C, A × D, and A × E. Because five factors at three levels and four interactions are considered, the orthogonal array L_{27} (3^{13}) is selected for our experiment.

In addition to the five factors, other factors could be changed during the test, which will affect the mechanical properties of the parts, in order to reduce the influence of these random factors as far as possible on the test results. Three identical test specimens are built for each case, which resulted in a total of 81 test specimens for $L_{27}3^{13}$ orthogonal array settings. The mean value of the three tests is calculated as the result. The microcomputer-controlled electronic universal testing machine (*WDW-10*) is used to measure the ultimate load (F) with cross-head speed of 2 mm/s as shown in Fig. 5. Then the tensile strength (σ_t) can be obtained by dividing the average ultimate load (F) by the cross-sectional area. The experiment results for tensile strength are shown in Table 3.

3.3.2 Experiment for flexural strength

The process of experiment for flexural strength is the same as experiment for tensile strength. Eighty-one specimens are built for orthogonal array L_{27} (3^{13}) setting of three replications each. Microcomputer control electronic universal testing machine is used for three-point bending test in Fig. 6. When the specimen deformation reaches to the specified deflection, the maximum bending stress can be called the flexural strength. The loading speed is 2 mm/min and the distance between two supports (L) is 30 mm.

Fig. 3 Test specimen for tensile strength experiment

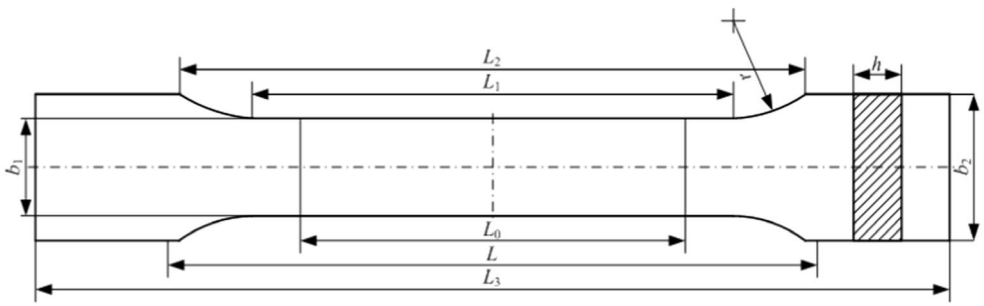

Table 2 Dimensions of tensile specimen

Symbol	Dimensions (mm)
L	115 ± 1
L_0	50 ± 0.5
L_1	80 ± 2
L_2	104–113
L_3	≥150
b_1	10 ± 0.2
b_2	20 ± 0.2
h	4 ± 0.2
r	20–25

The flexural strength σ_f is calculated using the following equation:

$$\sigma_f = \frac{3PL}{2bh^2} \quad (1)$$

where P is maximum bending load in Newton; b is the breadth of the test specimen in millimeters; and d is the depth of the test specimen in millimeters. The experiment results for flexural strength are tabulated in Table 4.

3.3.3 Experiment for impact strength

The design of the experiment for impact strength is identical with the former ones. Eighty-one unnotched specimens are constructed for Charpy pendulum impact resistance test. The impact resistance of the material is the ability to resist fracture under impact load. In the test, the specimen placed vertically is subjected to quick and intense blow by a single swing of the pendulum weight in Fig. 7. The absorbed impact energy is the measure of the material toughness and can be calculated by taking the difference in potential energy of initial and final position of swing.

The impact strength σ_i is obtained through the equation:

$$\sigma_i = \frac{A}{bh} \times 10^3 \quad (2)$$

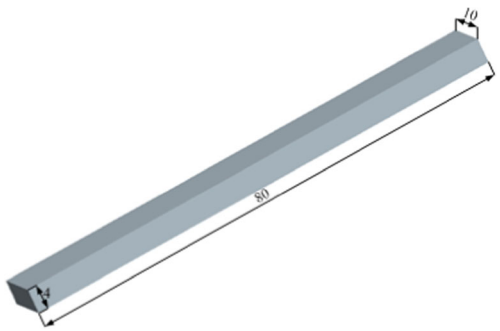

Fig. 4 The three-dimensional model of flexural test specimen

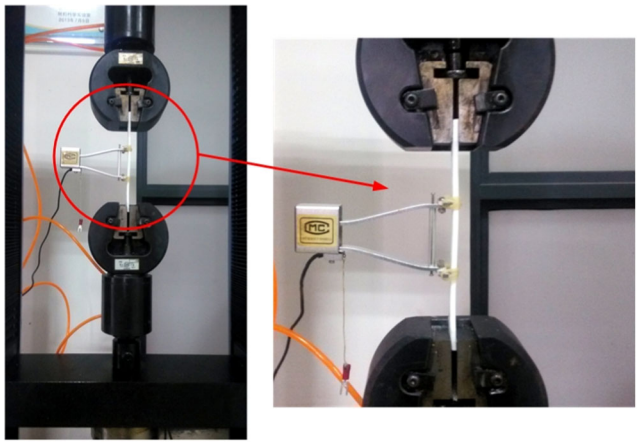

Fig. 5 *WDW*-10 microcomputer control electron universal testing machine

where A is the impact energy absorbed; b is the breadth of the test specimen in millimeters; and d is the depth of the test specimen in millimeters. The experiment results for impact strength are shown in Table 5.

3.4 Experiment result

With the Taguchi method, parameter design converts the objective value to S/N ratio, which is known as a

Table 3 Results of tensile experiment

Exp. no	Factors					F (KN)	σ_t (MPa)
	A	B	C	D	E		
1	1	1	1	1	1	1.83	45.52
2	1	1	2	2	2	1.65	41.19
3	1	1	3	3	3	1.74	43.53
4	1	2	1	2	3	1.94	48.54
5	1	2	2	3	1	1.66	41.49
6	1	2	3	1	2	1.76	44.11
7	1	3	1	3	2	1.97	49.18
8	1	3	2	1	3	1.70	42.38
9	1	3	3	2	1	1.82	45.57
10	2	1	1	1	1	1.70	42.57
11	2	1	2	2	2	1.53	38.18
12	2	1	3	3	3	1.58	39.50
13	2	2	1	2	3	1.75	43.81
14	2	2	2	3	1	1.62	40.47
15	2	2	3	1	2	1.67	41.67
16	2	3	1	3	2	1.79	44.64
17	2	3	2	1	3	1.66	41.57
18	2	3	3	2	1	1.74	43.47
19	3	1	1	1	1	1.54	38.51
20	3	1	2	2	2	1.39	34.63
21	3	1	3	3	3	1.49	37.22
22	3	2	1	2	3	1.68	42.08
23	3	2	2	3	1	1.66	41.42
24	3	2	3	1	2	1.59	39.84
25	3	3	1	3	2	1.75	43.70
26	3	3	2	1	3	1.64	41.04
27	3	3	3	2	1	1.67	41.78

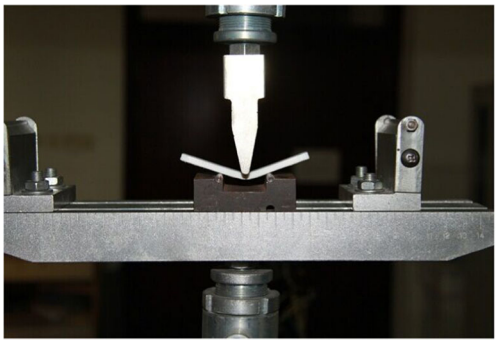

Fig. 6 Microcomputer control electronic universal testing machine for flexural experiment

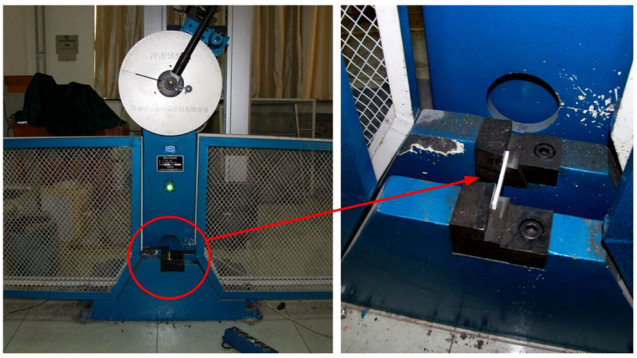

Fig. 7 Charpy pendulum impact resistance test

quality characteristic evaluation index [22, 23]. By means of the S/N ratio, the least variation and the optimal quality design can be obtained. The S/N ratio is beneficial in increasing factor weighting effect, decreasing mutual action, simultaneously processing the average and variation, and improving the quality. The objective of this paper is to maximize the mechanical properties of the part. Therefore, the larger-the-better characteristic is used. Its S/N ratio (η) can be calculated as follows:

$$\eta = -10\log\left[\frac{1}{p}\sum_{i=1}^{p}\frac{1}{w_i^2}\right] \tag{3}$$

where η is the S/N ratio; w_i is the ith result of the experiment; and p is the repeated times of a trial.

The three experimental results in S/N ratio are shown in Table 6; η_1, η_2, and η_3 are the S/N ratio for tensile strength, flexural strength, and impact strength, respectively.

Table 4 Results of flexural experiment

Exp. no	Factors					P (N)	σ_f (MPa)
	A	B	C	D	E		
1	1	1	1	1	1	308.06	86.64
2	1	1	2	2	2	303.04	85.23
3	1	1	3	3	3	320.47	90.13
4	1	2	1	2	3	303.33	85.31
5	1	2	2	3	1	306.31	86.15
6	1	2	3	1	2	282.07	79.33
7	1	3	1	3	2	295.04	82.98
8	1	3	2	1	3	257.35	72.38
9	1	3	3	2	1	263.15	74.01
10	2	1	1	1	1	282.17	79.36
11	2	1	2	2	2	255.90	71.97
12	2	1	3	3	3	248.36	69.85
13	2	2	1	2	3	257.03	72.29
14	2	2	2	3	1	264.11	74.28
15	2	2	3	1	2	245.37	69.01
16	2	3	1	3	2	261.76	73.62
17	2	3	2	1	3	241.50	67.92
18	2	3	3	2	1	237.98	66.93
19	3	1	1	1	1	218.46	61.44
20	3	1	2	2	2	205.90	57.91
21	3	1	3	3	3	228.73	64.33
22	3	2	1	2	3	210.74	59.27
23	3	2	2	3	1	198.26	55.76
24	3	2	3	1	2	192.11	54.03
25	3	3	1	3	2	201.50	56.67
26	3	3	2	1	3	182.44	51.31
27	3	3	3	2	1	188.02	52.88

Table 5 Results of impact experiment

Exp. no	Factors					A (J)	σ_i (kJ/m^2)
	A	B	C	D	E		
1	1	1	1	1	1	0.870	21.75
2	1	1	2	2	2	0.873	21.83
3	1	1	3	3	3	0.897	22.43
4	1	2	1	2	3	0.896	22.40
5	1	2	2	3	1	0.893	22.33
6	1	2	3	1	2	0.926	23.15
7	1	3	1	3	2	0.931	23.28
8	1	3	2	1	3	0.927	23.18
9	1	3	3	2	1	0.954	23.85
10	2	1	1	1	1	0.892	22.30
11	2	1	2	2	2	0.877	21.93
12	2	1	3	3	3	0.861	21.53
13	2	2	1	2	3	0.864	21.60
14	2	2	2	3	1	0.891	22.28
15	2	2	3	1	2	0.885	22.13
16	2	3	1	3	2	0.959	23.98
17	2	3	2	1	3	0.943	23.58
18	2	3	3	2	1	0.944	23.60
19	3	1	1	1	1	0.850	21.25
20	3	1	2	2	2	0.862	21.55
21	3	1	3	3	3	0.868	21.70
22	3	2	1	2	3	0.852	21.30
23	3	2	2	3	1	0.859	21.48
24	3	2	3	1	2	0.863	21.58
25	3	3	1	3	2	0.932	23.30
26	3	3	2	1	3	0.915	22.88
27	3	3	3	2	1	0.933	23.33

Table 6 Final result in S/N ratio

Exp. no	Factors					S/N ratio η (dB)		
	A	B	C	D	E	η_1	η_2	η_3
1	1	1	1	1	1	33.16	38.75	26.75
2	1	1	2	2	2	32.30	38.61	26.78
3	1	1	3	3	3	32.78	39.10	27.01
4	1	2	1	2	3	33.72	38.62	27.00
5	1	2	2	3	1	32.36	38.71	26.98
6	1	2	3	1	2	32.89	37.99	27.29
7	1	3	1	3	2	33.84	38.38	27.34
8	1	3	2	1	3	32.54	37.19	27.30
9	1	3	3	2	1	33.17	37.39	27.55
10	2	1	1	1	1	32.58	37.99	26.97
11	2	1	2	2	2	31.64	37.14	26.82
12	2	1	3	3	3	31.93	36.88	26.66
13	2	2	1	2	3	32.83	37.18	26.69
14	2	2	2	3	1	32.14	37.42	26.96
15	2	2	3	1	2	32.40	36.78	26.90
16	2	3	1	3	2	32.99	37.34	27.60
17	2	3	2	1	3	32.38	36.64	27.45
18	2	3	3	2	1	32.76	36.51	27.46
19	3	1	1	1	1	31.71	35.77	26.55
20	3	1	2	2	2	30.79	35.26	26.67
21	3	1	3	3	3	31.42	36.17	26.73
22	3	2	1	2	3	32.48	35.46	26.57
23	3	2	2	3	1	32.34	34.93	26.64
24	3	2	3	1	2	32.01	34.65	26.68
25	3	3	1	3	2	32.81	35.07	27.35
26	3	3	2	1	3	32.26	34.20	27.19
27	3	3	3	2	1	32.42	34.47	27.36

Furthermore, the ANOVA can be adopted to identify the importance of degree of factors and interactions to the strength of test specimens. The following equation can be used to calculate the parameters for ANOVA.

The total sum of square deviation (*SST*) and total degree of freedom (f_T) can be calculated as follows:

$$SST = \sum_{i=1}^{n} \eta_i^2 - \frac{T^2}{n}. \tag{4}$$

$$f_T = n-1. \tag{5}$$

Table 7 ANOVA table for tensile strength

Source	DOF	Sum of square	Variance	*F* value	Percentage contribution
A	2	4.08435	2.04217	60.79	0.001
B	2	2.77969	1.38984	41.37	0.002
C	2	3.06059	1.53029	45.55	0.002
D	2	0.02714	0.01357	0.40	0.692
E	2	0.05861	0.02930	0.87	0.485
A × B	4	0.59286	0.14821	4.41	0.090
A × C	4	0.32427	0.08107	2.41	0.207
A × D	4	0.18019	0.04505	1.34	0.392
Error	4	0.13437	0.03359	–	–
Total	26	11.24207	–	–	–

Table 8 ANOVA table for flexural strength

Source	DOF	Sum of square	Variance	*F* value	Percentage contribution
A	2	46.9110	23.4555	271.07	0.000
B	2	4.0086	2.0043	23.16	0.006
C	2	1.5324	0.7662	8.85	0.034
D	2	1.0288	0.5144	5.94	0.063
E	2	0.0294	0.0147	0.17	0.849
A × B	4	0.5432	0.1358	1.57	0.336
A × D	4	0.3733	0.0933	1.08	0.472
A × E	4	0.3555	0.0889	1.03	0.490
Error	4	0.3461	0.0865	–	–
Total	26	55.1284	–	–	–

The sum of square deviation of *j*th factor (SS_j) and its degree of freedom (f_j) can be calculated as follows:

$$SS_j = \frac{1}{r}\sum_{i=1}^{m} T_i^2 - \frac{T^2}{n} (j = 1, 2, \ldots, k). \tag{6}$$

$$f_j = m-1. \tag{7}$$

The sum of square of error (*SSE*) and its degree of freedom (f_e) can be calculated as follows:

$$SSE = SST - \sum_{j=1}^{k} SS_j. \tag{8}$$

$$f_e = f_T - \sum_{j=1}^{k} f_j. \tag{9}$$

The variance of *j*th parameter (MS_j) and the variance of error (*MSE)* can be calculated as follows:

$$MS_j = SS_j \Big/ f_j. \tag{10}$$

Table 9 ANOVA table for impact strength

Source	DOF	DOF	Variance	*F* value	Percentage contribution
A	2	0.31828	0.15914	21.74	0.007
B	2	2.08621	1.04310	142.48	0.000
C	2	0.05302	0.02651	3.62	0.127
D	2	0.00723	0.00362	0.49	0.643
E	2	0.03945	0.01972	2.69	0.182
A × B	4	0.13316	0.03329	4.55	0.086
A × C	4	0.11255	0.02814	3.84	0.110
A × E	4	0.03935	0.00984	1.34	0.391
error	4	0.02928	0.00732	–	–
total	26	2.81852	–	–	–

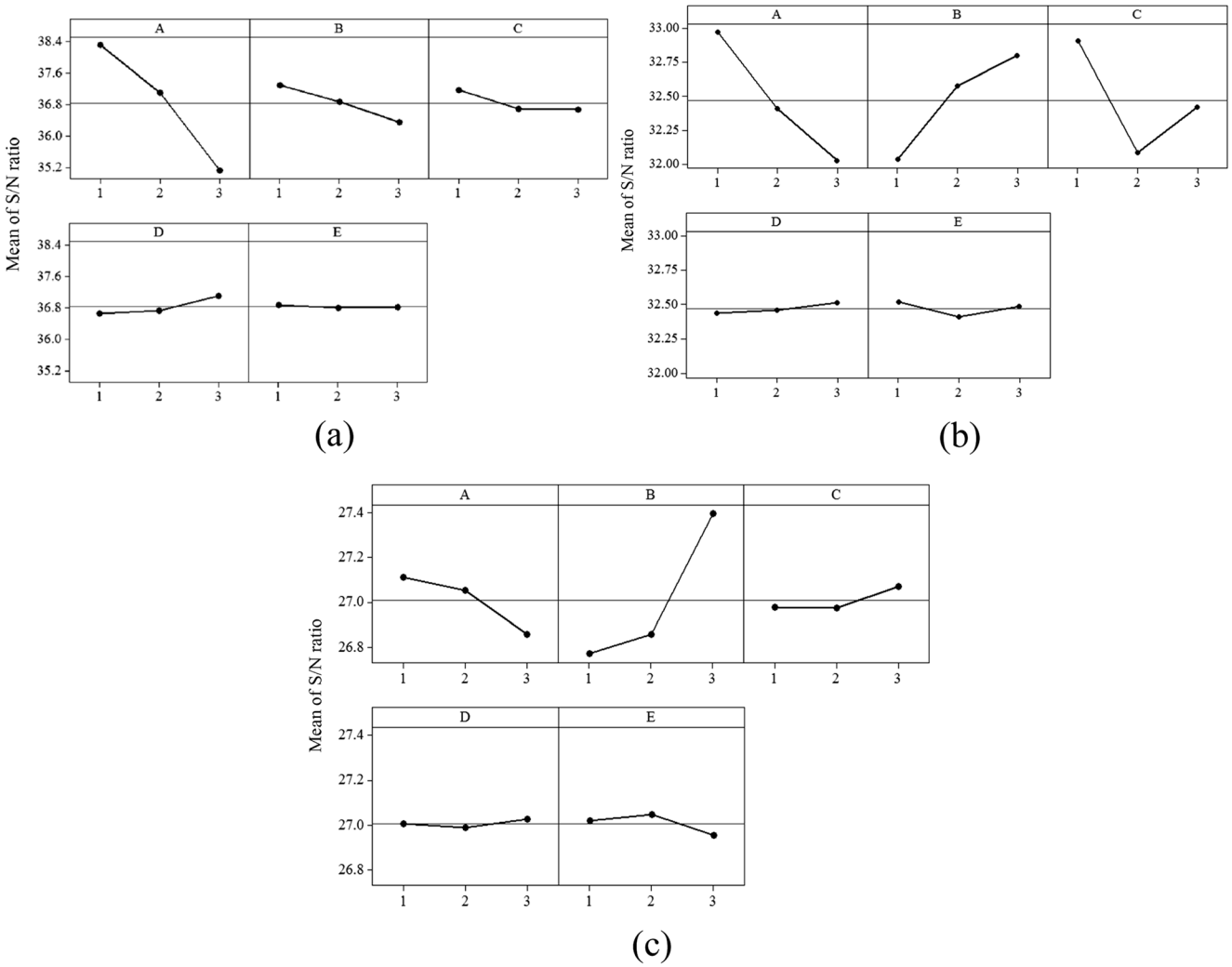

Fig. 8 Main effect plot for S/N ratio. **a** Tensile strength. **b** Flexural strength. **c** Impact strength

$$MSE = SSE \Big/ f_e. \tag{11}$$

F ratio of jth factor can be calculated as follows:

$$F_j = MS_j \Big/ MSE \tag{12}$$

where n is the total number of experiments, m is the number of levels for each factor, k is the number of columns of orthogonal array, $r = n/m$, T is the total sum of S/N ratio, and T_i is the sum of S/N ratio when the level of factors is fixed on ith row for an arbitrary column.

Relative influence of factors and interactions is determined by ANOVA [24], and the ANOVA results are presented in Tables 7, 8, and 9 for tensile, flexural, and impact strengths, respectively. The optimum levels of five main factors for each response of the part can be obtained intuitively from the main effect plot for S/N ratio in Fig. 8. Optimum factor levels with significant factors and interactions for the part strength are listed in Table 10.

4 Optimization of parameters combination with the gray relational analysis

In actual practice, the FDM parts are subjected to various types of loadings and it is necessary to withhold more than one mechanical property simultaneously. To address

Table 10 Optimum factor levels with significant factors and interactions

Factors	Tensile strength	Flexural strength	Impact strength
A	1	1	1
B	3	1	3
C	1	1	3
D	3	3	3
E	1	1	2
Significant	A, B, C	A, B, C	A, B

Table 11 Results of gray relational analysis

Exp. no	Gray relational generation			Gray relation coefficient			Gray relation grade
1	0.777	0.929	0.190	0.692	0.875	0.382	0.649
2	0.495	0.900	0.219	0.498	0.833	0.390	0.573
3	0.652	1.000	0.438	0.590	1.000	0.471	0.686
4	0.961	0.902	0.429	0.927	0.836	0.467	0.743
5	0.515	0.920	0.410	0.507	0.863	0.459	0.609
6	0.689	0.773	0.705	0.616	0.688	0.629	0.644
7	1.000	0.853	0.752	1.000	0.773	0.669	0.813
8	0.574	0.610	0.714	0.540	0.562	0.636	0.579
9	0.780	0.651	0.952	0.695	0.589	0.913	0.732
10	0.587	0.773	0.400	0.548	0.688	0.455	0.563
11	0.279	0.600	0.257	0.409	0.556	0.402	0.455
12	0.374	0.547	0.105	0.444	0.525	0.358	0.442
13	0.669	0.608	0.133	0.602	0.561	0.366	0.509
14	0.443	0.657	0.390	0.473	0.593	0.451	0.505
15	0.528	0.527	0.333	0.514	0.514	0.429	0.485
16	0.721	0.641	1.000	0.642	0.582	1.000	0.741
17	0.521	0.498	0.857	0.511	0.499	0.778	0.595
18	0.646	0.471	0.867	0.585	0.486	0.789	0.620
19	0.302	0.320	0.000	0.417	0.424	0.333	0.391
20	0.000	0.216	0.114	0.333	0.390	0.361	0.361
21	0.207	0.402	0.171	0.387	0.455	0.376	0.406
22	0.554	0.257	0.019	0.529	0.402	0.338	0.422
23	0.508	0.149	0.086	0.504	0.370	0.354	0.409
24	0.400	0.092	0.124	0.455	0.355	0.363	0.391
25	0.662	0.178	0.762	0.597	0.378	0.677	0.550
26	0.482	0.000	0.610	0.491	0.333	0.561	0.462
27	0.534	0.055	0.771	0.518	0.346	0.686	0.516

Table 12 ANOVA table for gray relational grade

Source	DOF	Sum of square	Variable	*F* value	Contribution percentage
A	2	64.5043	32.2521	184.07	0.000
B	2	19.0048	9.5024	54.23	0.001
C	2	8.1168	4.0584	23.16	0.006
D	2	1.6141	0.8070	4.61	0.092
E	2	0.3837	0.1918	1.09	0.418
A × B	4	3.5469	0.8867	5.06	0.073
A × C	4	2.2483	0.5621	3.21	0.143
A × D	4	1.0996	0.2749	1.57	0.337
Error	4	0.7009	0.1752	–	–
Total	26	101.2194	–	–	–

this issue, the gray relational analysis has been adopted to optimize more than one response at a time [25, 26]. The gray relational analysis is a quantitative analysis on exploring the similarity and dissimilarity among factors [27]. It uses the gray relational grade to find the correlation degree of factors.

4.1 Gray relational generating

In the GRA, the first step is to perform the normalization of experimental data to make the range within 0 to 1. This step is called gray relational generating (GRG) [28, 29]. The GRG also expresses the deviation between the experimental value and the ideal value. According to objective of quality characteristics, there are three criterions for optimization in gray relational analysis, namely "larger-the-better," "smaller-the-better," and "nominal-the-best." Assume that there are m alternatives and n attributes (in this paper, $m = 27$; $n = 3$), the ith alternative can be expressed as Y_i (y_{i1}, y_{i2},…, y_{ij},..., y_{in}), where y_{ij} is

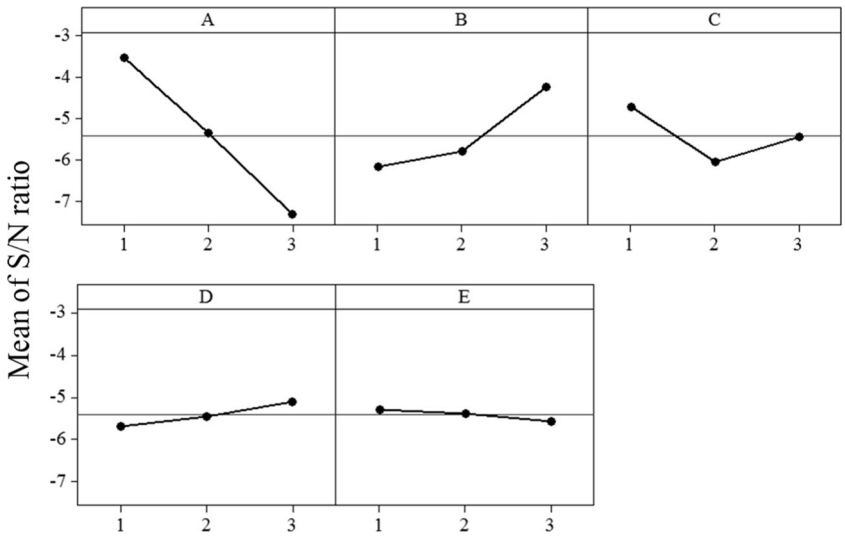

Fig. 9 Factor effect graph for gray relation grade

Table 13 Experimental results with optimal combination of process parameters

Factors					σ_t (MPa)	σ_f (MPa)	σ_i (kJ/m^2)	Γ
A	B	C	D	E				
1	3	1	3	1	50.34	83.51	23.07	0.857

the performance value of attribute j of alternative i. The larger-the-better of the GRA is used to normalize the term X_i through the following equation:

$$x_{ij} = \frac{y_{ij} - \min\limits_j y_{ij}}{\max\limits_j y_{ij} - \min\limits_j y_{ij}} (i = 1, 2, \ldots, m; j = 1, 2, \ldots, n) \quad (13)$$

where y_{ij} is the original value; and x_{ij} is the value after the gray relation generating process.

4.2 Gray relational coefficient

The gray relational coefficient λ is determined to express the relationship between reference and actual experimental normalized data. Thus, a reference sequence $X_0 = (x_{01}, x_{02}, \ldots, x_{0j}, \ldots, x_{0n})$ $(x_{0j} = 1,\ 1 \le j \le n)$ is used to compare comparability sequence. The gray relational coefficient λ can be calculated as follows:

$$\lambda(x_{0j}, x_{ij}) = \frac{\Delta_{\min} + \xi\Delta_{\max}}{\Delta_{ij} + \xi\Delta_{\max}} (i = 1, 2, \ldots, m; j = 1, 2, \ldots, n) \quad (16)$$

where $\Delta_{ij} = |x_{0j} - x_{ij}|$; and ξ is the distinguishing coefficient and its value lies between 0 and 1. Usually, the distinguishing coefficient is set as 0.5 to fit the practical requirements; $\Delta_{\min} = \min\{\Delta_{ij}, i = 1, 2, \cdots, m; j = 1, 2, \cdots, n\}$; $\Delta_{\max} = \max\{\Delta_{ij}, i = 1, 2, \cdots, m; j = 1, 2, \cdots, n\}$.

4.3 Gray relational grade

After calculating the entire gray relational coefficient, the gray relational grade Γ can be calculated using Eq. (17).

$$\Gamma(x_0, X_i) = \sum_{j=1}^{n} w_j \lambda(x_{0j}, x_{ij}) (i = 1, 2, \ldots, m; j = 1, 2, \ldots, n) \quad (17)$$

where w_j is the weight of attribute j and depends on the decision maker's judgment or the structure of the proposed problem. In addition, $\sum\limits_{j=1}^{n} w_j = 1$. In this work, the weights for percentage change in tensile strength, flexural strength, and impact strength are set as 0.333, 0.333, and 0.333, respectively. The results based on gray relational analysis are shown in Table 11.

4.4 Results and analysis

Through the gray relational analysis method, the three main indexes of the mechanical properties of the parts are finally quantified as a set of gray relational grade. The gray relational grade indicates the degree of similarity between the reference sequence and comparability sequence. If a comparability sequence for an alternative gets the highest gray relational grade, it will be most similar to reference sequence and the alternative would be the best choice. Thus, the maximization of gray relation grade gives the optimum factor levels [30]. In order to obtain the final significant factors and optimal process parameters for comprehensive mechanical property, S/N ratio and ANOVA were applied. The results are shown in Fig. 9 and Table 12. The main factor plot (Fig. 9) for gray relation grade gives factor level as A_1, B_3, C_1, D_3, E_1 are the optimal process parameters for the three mechanical properties of molding parts. And ANOVA on gray relation grade (Table 12) shows that factors A, B, and C are significant factors. To be exact, factor A is the most significant factor, followed by factor B, the last is factor C.

4.5 Experiment verification

Three specimens were designed based on the optimal combination of process parameters. The tensile, flexural, and impact strengths were measured by the corresponding test machine. The experimental results are shown in Table 13.

The data in Table 13 was compared with the result of no. 7 in Table 11, and it is found that the gray relational degree of prototype test increased from 0.813 to 0.857. That is to say, under the same experimental conditions, the optimal combination of process parameters based on gray relational analysis can achieve the best comprehensive mechanical properties of molded parts.

5 Conclusions and scope for future research

In this paper, the tensile strength, flexural strength, and impact strength of molding parts were considered as the evaluation indexes to characterize the mechanical properties. The orthogonal test of five factors and three levels was designed, and the Taguchi method was used to optimize and study the influence of various process parameters on the three performance indexes. Furthermore, the combination of five process parameters was obtained based on the gray relation analysis method and analysis of variance to acquire optimal comprehensive mechanical properties of molding parts.

However, the mechanical properties of FDM parts are only analyzed from a macro perspective in this paper. From the micro perspective, a further study is needed to explore the influence of process parameters on the internal organization structure mechanism of the forming parts.

Acknowledgments The support of the National Natural Science Foundation of Jiangsu Province (no. BK20151144), Discipline Frontier Research Project (no. 2015XKQY10), and Priority Academic Program Development of Jiangsu Higher Education Institutions (PAPD) in carrying out this research is gratefully acknowledged.

References

1. Chua CK, Leong KF, Lim CS (2010) Rapid prototyping: principles and applications. World Scientific publishing Co. Pte.Ltd
2. Yan X, Gu P (1996) A review of rapid prototyping technologies and systems. Comput Aided Des 28(4):307–318
3. Petzold R, Zeilhofer HF, Kalender WA (1999) Rapid prototyping technology in medicine—basics and applications. Comput Med Imaging Graph 23(5):277–284
4. Boschetto A, Giordano V, Veniali F (2012) Modelling micro geometrical profiles in fused deposition process. Int J Adv Manuf Technol 61(9–12):945–956
5. Upcraft S, Fletcher R (2003) The rapid prototyping technologies. Rapid Prototyp J 23(4):318–330
6. Zein I, Hutmacher DW, Tan KC, Teoh SW (2002) Fused deposition modeling of novel scaffold architectures for tissue engineering application. Biomaterials 23(4):1169–1185
7. Peng A, Xiao XM, Yue R (2014) Process parameter optimization for fused deposition modeling using response surface methodology combined with fuzzy inference system. Int J Adv Manuf Technol 73(1–4):87–100
8. Os ES, Foyos J, Noorani R, Mandelson M, Marloth R, Pregger BA (2000) Effect of layer orientation on mechanical properties of rapid prototyped samples. Mater Manuf Process 15(1):107–122
9. Hutmacher DW, Schantz T, Zein I et al (2001) Mechanical properties and cell cultural response of polycaprolactone scaffolds designed and fabricated via fused deposition modeling. J Biomed Mater Res 55(2): 203–216
10. Ahn SH, Montero M, Odell D, Roundy S, Wright PK (2002) Anisotropic material properties of fused deposition modeling ABS. Rapid Prototyp J 8(4):248–257
11. Lee CS, Kim SG, Kim HJ, Ahn SH (2007) Measurement of anisotropic compressive strength of rapid prototyping parts. J Mater Process Technol 187(12):627–630
12. Bellehumeur CT, Gu P, Sun Q, Rizvi GM (2008) Effect of processing conditions on the bonding quality of FDM polymer filaments. Rapid Prototype J 14(2):72–80
13. Jaya Christiyana KG, Chandrasekharb U, Venkateswarluc K (2016) A study on the influence of process parameters on the mechanical properties of 3D printed ABS composite. Mater Sci Eng 114(01):1–6
14. Khan ZA, Lee BH, Abdullah J (2005) Optimization of rapid prototyping parameters for production of flexible ABS object. J Mater Process Technol 169(2):54–61
15. Croccolo D, De Agostinis M, Olmi G (2013) Experimental characterization and analytical modeling of the mechanical behavior of fused deposition processed parts made of ABS-M30. Comput Mater Sci 79(6):506–518
16. Kotlinski J (2014) Mechanical properties of commercial rapid prototyping materials. Rapid Prototyp J 20(6):499–510
17. Kumar Sood A, Ohdar RK, Mahapatra SS (2010) Parametric appraisal of mechanical property of fused deposition modeling processed parts. Mater Des 31(1):287–295
18. Tymrak BM, Kreiger M, Pearce JM (2014) Mechanical properties of components fabricated with open-source 3-D printers under realistic environmental conditions. Mater Des 58(6):242–246
19. Hefin R, Jiju A, Graeme K (2000) An application of experimental design for process optimization. Rapid Prototyp J 12(2):78–84
20. Smith WC, Dean RW (2013) Structural characteristics of fused deposition modeling polycarbonate material. Polym Test 32(8): 1306–1312
21. Durgun I, Ertan R (2014) Experimental investigation of FDM process for improvement of mechanical properties and production cost. Rapid Prototyp J 20(3):228–235
22. Taguchi G (1990) Introduction to quality engineering. Asian Productivity Organization, Tokyo
23. Liu X, Li S, Zhou L et al (2015) An investigation on distortion of PLA thin-plate part in the FDM process. Int J Adv Manuf Technol 79(5):1117–1126
24. Peace Glen Stuart (1993) Taguchi methods: a hand on approach. Addison Wesley, New York
25. Kuo CFJ, Wu YS (2006) Optimization of the film coating process for polymer blends by the grey-based Taguchi method. Int J Adv Manuf Technol 27(5):525–530
26. Adalarasan R, Santhanakumar M, Rajmohan M (2015) Application of grey Taguchi-based response surface methodology (GT-RSM) for optimizing the plasma arc cutting parameters of 304L stainless steel. Int J Adv Manuf Technol 78(5–8):1161–1170
27. Kung CY, Wen KL (2007) Applying grey relational analysis and grey decision-making to evaluate the relationship between company attributes and its financial performance—a case study of venture capital enterprises in Taiwan. Decis Support Syst 43(3):842–852
28. Tzenga CJ, Linb YH, Yanga YK, Jeng MC (2009) Optimization of turning operations with multiple performance characteristics using the Taguchi method and grey relational analysis. J Mater Proc Technol 20 9(6):2753–2759
29. Chiang Y-M, Hsieh HH (2009) The use of the Taguchi method with grey relational analysis to optimize the thin-film sputtering process with multiple quality characteristic in color filter manufacturing. Comput Ind Eng 56(2):648–661
30. Kuo Y, Yang T, Huang GW (2008) The use of grey-based Taguchi method to optimize multi-response simulation problems. Eng Optim 40(6):517–528